

## Transport at the Air/Water Interface is the Reason for Rings in Protein Microarrays

Yang Deng and X.-Y. Zhu\*

*Department of Chemistry, University of Minnesota, Minneapolis, Minnesota 55455*

Taryn Kienlen and Athena Guo

*MicroSurfaces, Inc., 4001 Stinson Boulevard, Suite 430, Minneapolis, Minnesota 55421*

Received November 10, 2005; E-mail: zhu@chem.umn.edu

Following the success of DNA microarrays in genomics research, protein microarrays (including peptide and antibody arrays) are becoming important tools in proteomics. One of the most pressing issues in protein microarray technology is how to apply the technology quantitatively.<sup>1</sup> The difficulty in quantitative application results in a large part from the lack of understanding and control of the chemical and physical processes involved in probe immobilization. A protein microarray is usually made on a robotic spotter which deposits nanoliter to subnanoliter size droplets of protein solutions on a solid surface. After incubation and washing off excess solution, the microarray is used for probe–target interaction, and the result is most commonly detected via fluorescence imaging. A survey of protein microarray literature shows that one of the major reasons for poor reproducibility is nonuniform spot profile. In particular, spots on a protein, peptide, or antibody microarray often exhibit ring-like structures.<sup>2–5</sup> Despite their common occurrence, the mechanism for ring formation in protein microarrays is not understood. Formation of ring structures is well documented for thin films deposited on solid surfaces by the evaporation of a solution or suspension of a wide variety of materials;<sup>6–8</sup> the most commonly seen rings are coffee stains.<sup>9</sup> However, the mechanisms for these ring structures all involve drying and cannot be responsible for the ring structure seen in protein microarrays where the spots are kept hydrated.

A typical example of the ring structure is shown in Figure 1A for an antibody spot on an epoxy-terminated glass slide. After the deposition of nanoliter droplets of antibody solutions on the epoxy slide, we kept the sample in an environment with controlled humidity and confirmed using optical microscope that the size of each droplet on the surface did not change during incubation. A close examination of the morphology of the ring structure in Figure 1A, particularly, the cross-sectional profile of fluorescence intensity in Figure 1B, provides a clue. Within the ring, the fluorescence intensity peaks at the center and gradually decreases toward the boundary of the spot. Immediately outside the boundary, the concentration of immobilized antibody rises rapidly then decays with increasing distance from the boundary. To form such a concentration profile, protein molecules must be transported to the boundary outside of the droplet. Because the droplet remains stationary (no expansion or contraction) during incubation, we believe that transport of protein molecules occurs at the air–liquid interface. The proposed mechanism is shown schematically in Figure 1C. Protein molecules are known to preferentially accumulate at air/water interfaces.<sup>10,11</sup> Because the surface area-to-volume ratio scales with the inverse of droplet size, the equilibrium between solution phase protein and adsorbed protein at the air/liquid interface should greatly shift to the latter as the size of the droplet decreases from macroscopic to the nanoliter and subnanoliter scale. This effect

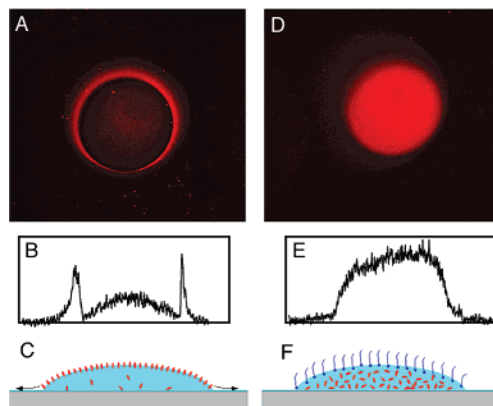


**Figure 1.** (A and D): Fluorescence microscope images of antibody (rabbit polyclonal anti-vanilloid receptor 1) spots immobilized on an epoxy-functionalized glass slide. In (A), a diluted antibody solution (1:500) was used directly, while in (D), a small amount detergent (0.006% Triton X-100) was added to the diluted antibody solution. The epoxy slide was prepared from exposing clean glass slides to 3-glycidyloxypropyl trimethoxysilane vapor. Antibody solutions were deposited on the epoxy slide via a robotic spotter (Molecular Dynamics, Array Spotter II). Each slide was incubated for 1 h in controlled humidity environment, washed three times with a buffer solution (PBS with 0.01% Tween 20), and blocked with 1% BSA in PBS. Each sample was then incubated with a dye-labeled secondary antibody solution (Cye 3-conjugated anti-rabbit) for 1 h, followed by PBS buffer wash three times. Fluorescence images were obtained on a Nikon 50i microscope with excitation at 550 nm. Panels (B) and (E) are cross-sectional profiles of images (A) and (D), respectively. Panels (C) and (F) are schematic illustrations of nanoliter droplets (light blue) on a solid surface (gray) with protein molecules in red and detergent molecules in dark blue. Diameter of each spot is  $\sim 0.1$  mm.

provides an efficient mechanism for transporting protein molecules to the perimeter of the droplet, thus giving rise to a high concentration of protein molecules at the boundary of the spot. Diffusion of protein molecules accumulated at the boundary to an area outside the spot accounts for the rapid decay in fluorescence intensity further away from the boundary (Figure 1A and B).

If the proposed mechanism is true, we should be able to eliminate the ring structure by adding competitive surfactants to displace protein molecules at the air/water interface<sup>10,11</sup> (see cartoon in Figure 1F). This is indeed observed. Figure 1D shows a fluorescence microscope image of the antibody spot obtained with a small amount of detergent (0.006% Triton X-100) added to the antibody solution (no significant change in contact angle), under otherwise identical conditions as in Figure 1A. Instead of the ring, we now observe nearly uniform intensity inside the spot, with negligible intensity outside the boundary (see also cross-sectional profile in Figure 1E). The integrated intensity of the spot in Figure 1D is 4 times that in Figure 1A (inside the ring). Even if we include the

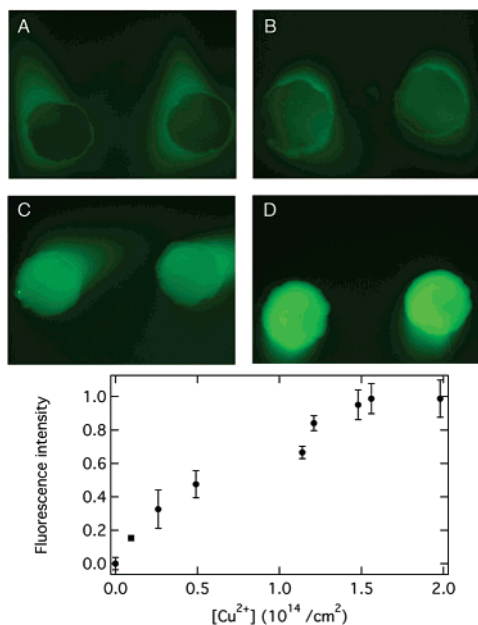


**Figure 2.** Fluorescence microscope images of 6xHis-tagged GFP immobilized on Cu<sup>2+</sup>-chelated polyether/glass surfaces with different surface Cu<sup>2+</sup> concentrations: (A)  $2.6 \times 10^{13}/\text{cm}^2$ ; (B)  $4.9 \times 10^{13}/\text{cm}^2$ ; (C)  $1.2 \times 10^{14}/\text{cm}^2$ ; and (D)  $2.0 \times 10^{14}/\text{cm}^2$ . Nanoliter droplets of crude lysate solution (4 mg/mL) containing 6xHis-GFP and 10% glycerol were deposited onto the glass slide by the robotic spotter. Each slide was incubated at room temperature for 10 min and rinsed quickly with PBS containing 0.01% Tween-20 three times. The slide was covered with the buffer solution and imaged under the fluorescence microscope (excitation wavelength  $\sim 488$  nm). The lower panel shows the fluorescence intensity within the spot as a function of surface [Cu<sup>2+</sup>] concentration. Diameter of each spot is  $\sim 0.1$  mm.

ring in integration, the total intensity of the spot in Figure 1A is still less than half of that in Figure 1D. In the absence of competitive surfactants, the accumulation of protein molecules at the air/water interface and the perimeter of the spot results in a depletion of protein concentration within the nanoliter droplet and, thus, a decreased immobilization efficiency. When protein molecules are displaced from the air/water interface by competitive surfactants, the concentration of protein solution in contact with the solid surface is the same as the concentration in the bulk sample. As a result, the immobilization efficiency is now directly related to protein concentration. This is also critical to the quantitative application of protein microarrays.

To further verify the mechanism of ring formation, we use a model system: the immobilization of 6x histidine-tagged green fluorescent protein (6xHis-GFP) on polyether ( $\sim 3$  nm)-coated glass slides with controlled density of chelated surface Cu<sup>2+</sup> ions (via surface-attached iminodiacetic acid groups). These surfaces are commercially available (MicroSurfaces, Inc., Minneapolis, USA) and are similar to that described in a previous publication.<sup>12</sup> The advantage of this system can be realized from the fact that intrinsic fluorescence is detected only when GFP is active under fully hydrated conditions, and any ring formation mechanism due to drying can be completely eliminated. The reaction between 6xHis tags and surface Cu<sup>2+</sup> sites is facile and highly selective. There is no protein adsorption in the absence of surface Cu<sup>2+</sup> or poly-His tags. Except for activated surface sites with chelated Cu<sup>2+</sup> ions, the other area on the polyether coating is repulsive toward protein adsorption. With increasing concentration of surface active sites, the surface becomes less repulsive, resulting in a shift in equilibrium toward adsorbed protein on the solid surface. Figure 2 shows fluorescence microscope images of 6xHis-GFP immobilized on the

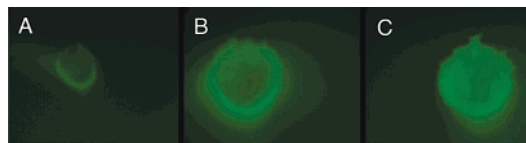


**Figure 3.** Fluorescence microscope images of 6xHis-tagged GFP immobilized on Cu<sup>2+</sup>-chelated polyether/glass surfaces with a surface Cu<sup>2+</sup> concentration of  $2.6 \times 10^{13}/\text{cm}^2$  and the addition of detergent (Triton X-100) to the protein solution: (A) 0.00, (B) 0.025, and (C) 0.100%.

surface with different concentrations of surface Cu<sup>2+</sup> as determined by X-ray photoelectron spectroscopy: (A)  $2.6 \times 10^{13}/\text{cm}^2$ ; (B)  $4.9 \times 10^{13}/\text{cm}^2$ ; (C)  $1.2 \times 10^{14}/\text{cm}^2$ ; and (D)  $2.0 \times 10^{14}/\text{cm}^2$ . As expected, the efficiency of protein immobilization (fluorescence intensity) within the spot increases as the density of surface reactive sites increases (bottom panel). For [Cu<sup>2+</sup>] less than  $\sim 5 \times 10^{13}/\text{cm}^2$  (panels A and B), fluorescence intensity inside the spot is less than that at or immediately outside the boundary, and the ring structure is observed. At higher [Cu<sup>2+</sup>] (panels C and D), the spot morphology becomes uniform. The finding of such a transformation in spot morphology illustrates the central role of kinetics in protein immobilization. For protein molecules within the nanoliter droplet, immobilization onto the surface and transport via the air/water interface to the spot boundary are two competing kinetic processes. In the 6xHis-GFP example shown here, transport dominates for low [Cu<sup>2+</sup>], while surface immobilization reaction kinetics wins at higher surface active site densities. Thus designing surface chemistry for a facile immobilization reaction is critical in ensuring uniform spot profiles. In the case of low surface [Cu<sup>2+</sup>] where the ring structure is observed for 6xHis-GFP immobilization, transformation to a more uniform spot profile also occurs with the addition of detergent into the protein solution (Figure 3). This is similar to the results for antibody immobilization in Figure 1. Note that, with the amount of surfactant added, there is a decrease in contact angle and an increase in spot size.

In summary, we demonstrate that the ring structure in spot morphology commonly seen in protein, peptide, or antibody microarrays results from the transport of protein molecules accumulated at the air/water interface to the perimeter of the droplet on a solid surface. The effect should become increasingly significant as the droplet size decreases. One can eliminate the ring structure by adding competitive surfactants to the protein solution or by designing facile surface reactions for protein immobilization.

**Acknowledgment.** Financial support from the National Institutes of Health (Grant No. 2R44RR017130) is acknowledged.

## References

- (1) Hanash, S., Ed. Special Issue: Protein microarrays. *Proteomics* **2003**, *3* (11 and all papers therein).
- (2) MacBeath, G.; Schreiber, S. L. *Science* **2000**, *289*, 1760.
- (3) Houseman, B. T.; Huh, J. H.; Kron, S. J.; Mrksich, M. *Nat. Biotechnol.* **2002**, *20*, 270.
- (4) Haab, B. B. *Proteomics* **2003**, *3*, 2116.
- (5) Angenendt, P.; Glöckler, J.; Sobek, J.; Lebrach, H.; Cahill, D. J. *J. Chromatogr. A* **2003**, *1009*, 97.
- (6) Schenning, A. P. H. J.; Benneker, F. B. G.; Geurts, H. P. M.; Liu, X. Y.; Nolte, R. J. M. *J. Am. Chem. Soc.* **1996**, *118*, 8549.
- (7) Hahn, J.; Sibener, S. J. *Langmuir* **2000**, *16*, 4766.
- (8) Ohara, P. C.; Heath, J. R.; Gelbart, W. M. *Angew. Chem., Int. Ed. Engl.* **1997**, *36*, 1078.
- (9) Deegan, R. D.; Bakajin, O.; Dupont, T. F.; Huber, G.; Nagel, S. R.; Witten, T. A. *Nature* **1997**, *389*, 827.
- (10) Clark, D. C.; Mackie, A. R.; Wilde, P. J.; Wilson, D. R. *Faraday Discuss.* **1994**, *98*, 253.
- (11) Mackie, A. R.; Gunning, A. P.; Wilde, P. J.; Morris, V. J. *J. Colloid Interface Sci.* **1999**, *210*, 157.
- (12) Cha, T.-W.; Guo, A.; Jun, Y.; Pei, D.-Q.; Zhu, X.-Y. *Proteomics* **2004**, *4*, 1965.

JA057669W